Hyperfine interaction measurements in $LaCrO_3$ and $LaFeO_3$ perovskites using perturbed angular correlation spectroscopy

R. Dogra,* A. C. Junqueira, R. N. Saxena, A. W. Carbonari,† J. Mestnik-Filho, and M. Moralles
Instituto de Pesquisas Energéticas e Nucleares IPEN-CNEN/SP, P.O. Box 11049 - Pinheiros, 05422-970 São Paulo, SP, Brazil
(Received 7 December 2000; published 10 May 2001)

The perturbed angular correlation (PAC) technique was used to study the hyperfine interactions in the antiferromagnetic and paramagnetic regions of the distorted perovskites $LaCrO_3$ and $LaFeO_3$. The dilute $^{111}In \rightarrow ^{111}Cd$ nuclear probes were introduced into the samples through a chemical process. The present measurements cover the temperature ranges from 15 to 848 K for $LaCrO_3$ and 77 to 1324 K for $LaFeO_3$. Two distinct electric-quadrupole interactions were observed in each compound. The lower quadrupole frequency was assigned to the transition-metal atom site while the higher frequency was attributed to the lanthanum site in both cases. Temperature dependence of the electric-quadrupole interaction parameters indicated structural phase transitions at around 512 and 1223 K, respectively, in $LaCrO_3$ and $LaFeO_3$. The phase transitions were associated with the change from an orthorhombic to rhombohedral structure and characterized by a sudden increase in the electric field gradient V_{zz} and a decrease in the asymmetry parameter η for both sites. PAC spectra measured below the Néel temperature revealed that at 0 K the supertransferred magnetic hyperfine field on ^{111}Cd at the Cr site in $LaCrO_3$ (2.4 T) is much smaller than at the Fe site in $LaFeO_3$ (19.4 T). The magnetic field on ^{111}Cd at La sites in both compounds is of the order of 0.3 T. Additional measurements were made to determine the magnetic hyperfine field using the probe nucleus $^{140}La \rightarrow ^{140}Ce$. The result reconfirmed that a relatively weak hyperfine field is supertransferred to the probe atoms at La sites.

DOI: 10.1103/PhysRevB.63.224104 PACS number(s): 76.80.+y, 71.90.+q, 31.30.Gs

I. INTRODUCTION

The perovskite oxides ABO_3 containing a rare-earth metal on A sites with twelvefold oxygen coordination and a transition metal on B sites with sixfold oxygen coordination are found to exhibit a rich variety of unusual and interesting electronic, magnetic, and structural properties. As a result these perovskites have gained much technological importance in the area of solid-state materials research. In general, the structure of perovskites of type ABO_3 is characterized as a cubic closest-packed array of oxygen anions and large A cations, with small B cations in the octahedral interstitial sites. The ideal cubic structure is distorted by cation size mismatch and distorted structures are mostly orthorhombic and rhombohedral. Goldschmidt[1] defined a tolerance factor $t=(A-O)/\sqrt{2}(B-O)$ to describe perovskite structures. The factor t is unity for an ideal cubic structure. For $t<1$ the space-group symmetry is lowered from cubic to tetragonal, rhombohedral, or orthorhombic. According to Glazer[2] for tolerance factors only slightly smaller than unity the formation of rhombohedral phase is favored if the BO_6 octahedron is considered to be rigid and the average B-O bond length is temperature independent. Therefore, A-O bonds are elongated with an increase in temperature and contribute mostly to the thermal expansion and hence the phase transformation. For larger deviations from the ideal ionic radius ratio, orthorhombic structure is observed. It is therefore interesting to observe the effect of temperature on cation-anion bond lengths with some suitable microscopic technique using appropriate probes at A and B sites. To study such effects, lanthanum orthochromite $LaCrO_3$ and lanthanum orthoferrite $LaFeO_3$ are good candidates as these perovskites are distorted and show temperature-dependent structural and magnetic phase transitions. At ambient temperature these compounds have an orthorhombically distorted perovskite structure[3] of the type $GdFeO_3$ and transform to rhombohedral structure at high temperature ($\sim$500 K for $LaCrO_3$ and $\sim$1200 K for $LaFeO_3$ perovskites) accompanied by large volume shrinkage involving absorption of heat.[4,5] Furthermore, at very high temperature ($>$1800 K), another phase transition, from rhombohedral to cubic structure,[3] has been observed. $LaCrO_3$ is a weak antiferromagnet below room temperature[6] while $LaFeO_3$ is a canted antiferromagnet with high transition temperature of about 743 K.[7]

Although the structural as well as magnetic phase-transition behavior of the $LaCrO_3$ and $LaFeO_3$ perovskites have been confirmed by other techniques,[3–6] only a few microscopic studies on atomic scale have been reported. Recent microscopic investigations of perovskites ABO_3 (Refs. 7–10) were carried out through determination of the electric field gradient (EFG) and magnetic hyperfine field (MHF) at probes located at A and B sites, by a perturbed angular correlation (PAC) technique. This method offers a high sensitivity to local structure variations in the crystal lattice and, consequently, can be used to follow changes such as bond distances, symmetry, defect trapping, etc. on a microscopic scale. Sample preparation is therefore the most important part in perovskite materials as defects can be produced that alter the characteristics of these materials. Recently, in order to attain homogeneity, stoichiometry and high density, several ceramic preparation techniques based on chemical routes such as the citrate gel process, coprecipitation, and the complex compound process have been employed. We have adopted one of the chemical processes to synthesize polycrystalline samples of $LaCrO_3$ and $LaFeO_3$, that offers a unique way to introduce the probe ions homogeneously in

 ©2001 The American Physical Society

the sample and this homogeneity is retained even after sintering at high temperature. Time differential perturbed angular correlation (TDPAC) measurements were performed in $LaCrO_3$ and $LaFeO_3$ perovskites at different temperatures using $^{111}In \rightarrow {}^{111}Cd$ probes to obtain information about the phase transition from orthorhombic to rhombohedral structure and the temperature dependence of the EFG and MHF at La, Cr, and Fe sites. Additional TDPAC measurements using $^{140}La \rightarrow {}^{140}Ce$ probes were also carried out below the Néel temperature for both compounds.

II. EXPERIMENTAL PROCEDURE

Stoichiometric polycrystalline samples of $LaCrO_3$ were prepared from a mixture of lanthanum nitrate and chromium nitrate solutions. The $La(NO_3)_3$ was prepared by dissolving a known quantity of La_2O_3 (99.9%) in concentrated HNO_3. The required quantity of $Cr(NO_3)_3.9H_2O$ (99%) was then added to the $La(NO_3)_3$ solution to obtain a homogeneous aqueous solution. Approximately 20–30 μCi of carrier-free ^{111}In was added and the whole solution was slowly evaporated to dryness. The resulting powder was pressed into small pellets and sintered for 5 h at 1300 K in air, ground to a powder, and sintered again at temperatures between 1600 and 1700 K for 5 h in air. The $LaFeO_3$ sample was prepared by a similar method where the starting materials La_2O_3 (99.9%) and metallic Fe (99.99%) were initially dissolved in concentrated HNO_3. Approximately 100 mg of $LaFeO_3$ and $LaCrO_3$, prepared without the addition of ^{111}In, were irradiated with neutrons in the IEA-R1 research reactor at the Instituto de Pesquisas Energéticas e Nucleares to produce the ^{140}La activity.

The powder samples of $LaCrO_3$ and $LaFeO_3$ were analyzed by the x-ray-diffraction method. The magnetization measurements on these samples were made using a superconducting quantum interference device (SQUID) magnetometer. The hyperfine interaction of the 245-keV $5/2^+$ spin state of the ^{111}Cd probe nuclei in the polycrystalline samples of $LaCrO_3$ and $LaFeO_3$ has been measured by the TDPAC technique utilizing the (171–245)-keV γ-γ cascade. The γ-γ cascade of (329–487) keV populated from the beta decay of ^{140}La was used for the measurement of magnetic interaction of the 2083-keV 4^+ spin state in ^{140}Ce. TDPAC spectra were recorded at several temperatures using a standard setup with four BaF_2 detectors arranged in a planar 90°–180° geometry, generating simultaneously 12 delayed coincidence spectra. The detector system had a time resolution of 800 ps. A small tube furnace was used for the measurements above room temperature and the temperature was controlled to within 2 K. For low-temperature measurements the sample was attached to the cold finger of a closed-cycle helium refrigerator with temperature controlled to better than 0.1 K. Spin rotation spectra $R(t)$ were generated from background subtracted coincidence counts $C(\theta,t)$,

$$R(t)=2\left[\frac{C(180°,t)-C(90°,t)}{C(180°,t)+2C(90°,t)}\right], \tag{1}$$

where $C(\theta,t)$ are the geometric mean of the coincidences taken from the spectra recorded at angle θ. Above the magnetic transition temperature, the measured perturbation function $R(t)$ was fitted by using the following model for the static nuclear-electric-quadrupole interaction:

$$R(t)=A_{22}G_{22}(t)=A_{22}\sum_i f_i G_{22}^i(t), \tag{2}$$

where A_{22} is the unperturbed angular correlation coefficient, f_i are the fractional site populations, and $G_{22}^i(t)$ are the corresponding perturbation factors given by

$$G_{22}(t)=S_{20}+\sum_{n=1}^{3} S_{2n}\cos(\omega_n t)\exp(-\omega_n^2\tau_R^2/2) \times \exp(-\omega_n^2\delta^2 t^2/2), \tag{3}$$

where the primary frequencies ω_n and their amplitudes S_{2n} are related to the hyperfine splitting of the intermediate nuclear level and depend on the nuclear quadrupole frequency $\omega_Q=eQV_{zz}/4I(2I-1)\hbar$ and the asymmetry parameter $\eta=(V_{xx}-V_{yy})/V_{zz}$, where V_{xx}, V_{yy}, and V_{zz} are the elements of the EFG tensor in its principal-axis system. As usual, V_{zz} is the largest component of the EFG tensor and generally one uses the spin-independent quadrupole frequency defined by $\nu_Q=eQV_{zz}/h$, where Q is the nuclear-electric-quadrupole moment of the intermediate level. The known quadrupole moment of 0.83 b for the $I=5/2^+$ intermediate level of ^{111}Cd has been used to determine V_{zz}. The effects of finite time resolution τ_R of detectors and the distribution of the EFG with a width δ are properly taken into account in Eq. (3).

In order to fit the perturbation functions measured at temperatures below the Néel temperature, we used a model for the combined electric and magnetic interactions in a polycrystalline sample from which the quadrupole frequency ν_Q as well as the Larmor frequency $\omega_L=g\mu_N B_{hf}/\hbar$ can be deduced, where g is the nuclear g factor and B_{hf} is the hyperfine magnetic field. The known value of the g factor $g=0.31$ for the $I=5/2^+$ intermediate level of ^{111}Cd was used to determine the hyperfine field B_{hf}.

III. EXPERIMENTAL RESULTS

The powder x-ray-diffraction patterns of the samples measured at room temperature were analyzed using the Rietveld method and confirmed a single phase in both compounds having orthorhombic structure with no contaminating phases (Fig. 1). The measured crystallographic lattice constants for lanthanum orthochromite ($LaCrO_3$) are $a=5.479$, $b=7.759$, and $c=5.513$ Å with space group *Pnma*, while for lanthanum orthoferrite ($LaFeO_3$), we obtained lattice parameters $a=5.553$, $b=7.857$, and $c=5.563$ Å, with the *Pbnm* space group showing good agreement with the earlier x-ray measurements.[6,11] The structure of an orthorhombically distorted perovskite ABO_3 is shown in Fig. 2. Magnetization measurements with a SQUID magnetometer confirmed the antiferromagnetic phase with Néel tempera-

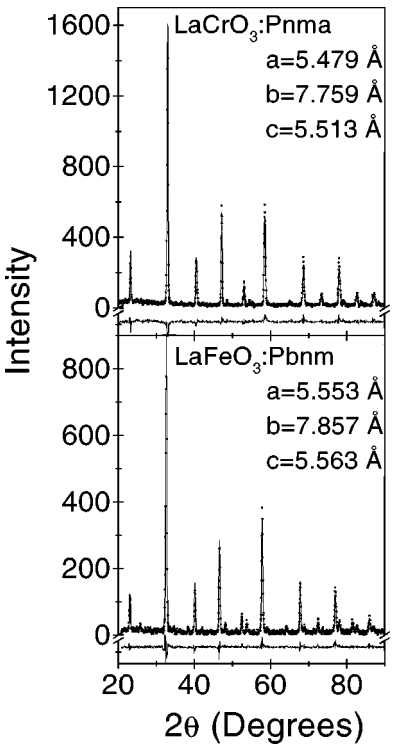

FIG. 1. The observed x-ray powder-diffraction spectra for $LaCrO_3$ and $LaFeO_3$ perovskite samples at room temperature at which both samples crystallize in orthorhombic structure. The solid lines represent the calculated pattern with the Rietveld method. The residuals are shown in the lower part of the curve.

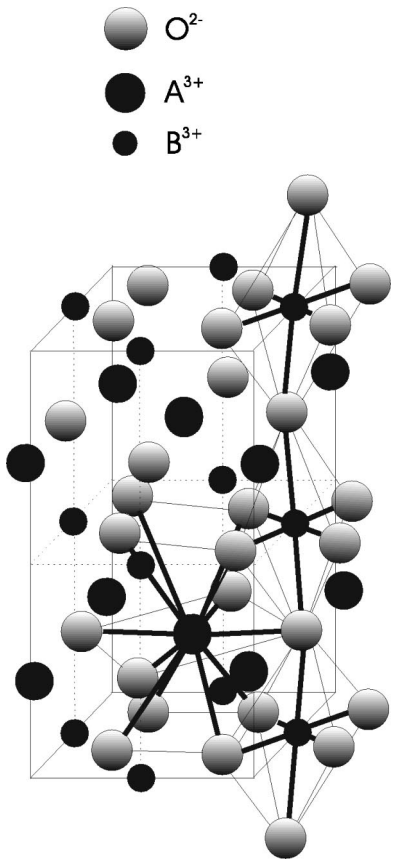

FIG. 2. Structure of an orthorhombically distorted perovskite ABO_3.

tures of 291(1) and 740(1) K, respectively, for $LaCrO_3$ and $LaFeO_3$ samples.

The perturbation functions, measured above the Néel temperature, for the $LaCrO_3$ and $LaFeO_3$ samples along with their respective Fourier transforms are shown in Figs. 3 and 4. The PAC spectra were least-squares fitted with up to three probe sites using the theoretical perturbation function given by Eq. (3). A visual inspection of the Fourier spectra clearly shows two major fractions with sharp and well-resolved frequencies in both compounds.

One of the major tasks of PAC experiments is to identify correctly the location of the nuclear probe in the crystal lattice, giving rise to the observed perturbation function. In both perovskites studied here, we have associated the observed higher quadrupole frequency $\nu_Q \sim 140$ MHz to the ^{111}Cd probe substituting the La atom and the lower frequency $\nu_Q \sim 30$ MHz to the probe substituting the Cr(Fe) atoms. This assignment is essentially based on the result of an earlier PAC measurement in several rare-earth (RE) orthoferrites including the $LaFeO_3$ (Ref. 7). The ^{111}In $\rightarrow ^{111}$Cd probe was introduced in these compounds by a similar chemical process as the one used in the present study (see Ref. 7 for details) and it was found that the probe atoms preferred to substitute both the RE as well as Fe sites, particularly in the orthoferrites containing lighter RE atoms, and that the MHF at the Fe site was larger compared to the RE atom site. Since, at higher temperatures, the magnetic ordering in these compounds involves primarily the Fe^{3+} ions through superexchange interactions via Fe^{3+}-O^{2-}-Fe^{3+} bonds, it was argued that the supertransferred field at the ^{111}Cd probe should be larger when it substitutes the Fe atom since the Fe-O-Fe(^{111}Cd) exchange bond angle is nearly 180° compared to the RE atom where the Fe-O-RE(^{111}Cd) exchange bond angle is close to 90°. Furthermore, a direct comparison of the PAC results with those of ^{57}Fe-Mössbauer measurements in these compounds[12] strongly suggested that the ^{111}Cd probe, substituting an Fe atom, is most likely to sense a large MHF but a small EFG, whereas the probe substituting a RE atom should sense a small MHF and a large EFG. Our PAC results of $LaFeO_3$, obtained both at 295 and 800 K ($T_N = 740$ K), are quite similar to those obtained by Rearick, Catchen, and Adams.[7] We therefore agree with the above assignment for the probe sites in $LaFeO_3$. The results of PAC measurements of $LaCrO_3$ show very similar features of electric-quadrupole and magnetic dipole interactions as in the case of $LaFeO_3$ and, therefore, strongly suggest the above assignments also for the ^{111}Cd probe in $LaCrO_3$.

We first present the results of the PAC measurements of $LaCrO_3$ and $LaFeO_3$ samples carried out above their Néel temperatures. As mentioned before, two major quadrupole frequencies were observed in each compound. The lower quadrupole frequencies are assigned to the Cr or Fe site while the higher frequencies correspond to ^{111}Cd probes at the La site. It has been further observed that the relative fractions of the probe nuclei at the La and Cr(Fe) sites are

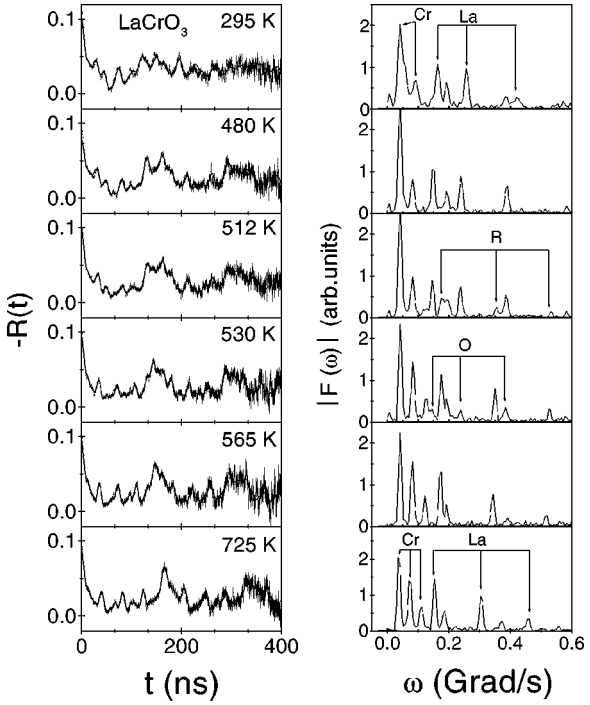

FIG. 3. The perturbation functions and their Fourier transforms for ^{111}Cd probes in $LaCrO_3$ at various temperatures. Solid lines are the least-squares fits of the theoretical function to the experimental data. Indicators *R* and *O* point to the frequency components assigned to the rhombohedral and the orthorhombic phases, respectively.

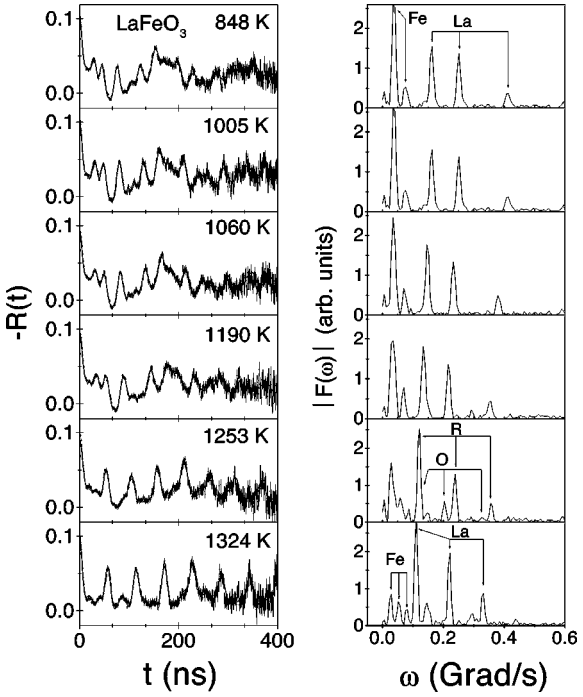

FIG. 4. The perturbation functions and their Fourier transforms for ^{111}Cd probes in $LaFeO_3$ at various temperatures. Solid lines are the least-squares fits of the theoretical function to the experimental data. Indicators *R* and *O* point to the frequency components assigned to the rhombohedral and the orthorhombic phases, respectively.

highly dependent on the temperature at which the sample is sintered. This effect is shown in Fig. 5 for $LaFeO_3$. While an increase in sintering temperature enhanced the La site fraction, a third unknown fraction appears at the expense of both La and Cr(Fe) site fractions and its population increases with the sintering temperature. At the sintering temperature of about 1620 K the minor fractions in both compounds are less than 5–7%. These minor fractions are characterized by $\nu_Q = 110$ MHz, $\eta = 1$ and $\nu_Q = 154$ MHz, $\eta = 0$, respectively, for $LaCrO_3$ and $LaFeO_3$ and do not show significant temperature dependence. We do not quite understand the origin of these unknown fractions.

It can be seen from Fig. 6, which shows the temperature dependence of the hyperfine parameters for $LaCrO_3$, that the η value for ^{111}Cd probe nuclei occupying Cr sites increases from 0.6 to 1.0 between 295 and 530 K indicating a large distortion of CrO_6 octahedra that increases with temperature. The corresponding η values for the La site are close to 0.5 and do not change in this temperature range. The large η values in both cases imply that the EFG principal axes at La and Cr sites are not aligned with the crystallographic axes. Much smaller values of η are observed for both sites at temperatures above 530 K. This sudden drop in the η value is due to a well-known[3–5] phase transition from orthorhombic to rhombohedral structure at about 512 K. The rhombohedral structure with a threefold rotation axis at La as well as at Cr sites is more symmetric than the orthorhombic structure. A small but nonzero value of η in the rhombohedral phase is an indication that the axial symmetry is not perfect, most probably, due to the presence of ^{111}Cd impurity probe atoms substituting Cr and La. In the vicinity of the temperature region 512–530 K, there is an abrupt increase in the values of the quadrupole interaction frequencies ν_Q to

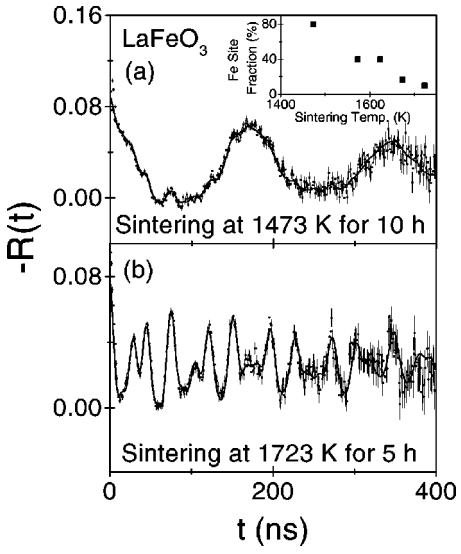

FIG. 5. Effect of sintering temperature on the site occupation of ^{111}Cd probes in $LaFeO_3$. The measured perturbation functions at 800 K are shown for the sample sintered at (a) 1473 and (b) 1723 K. The inset shows the variation of the Fe site fraction as a function of sintering temperature.

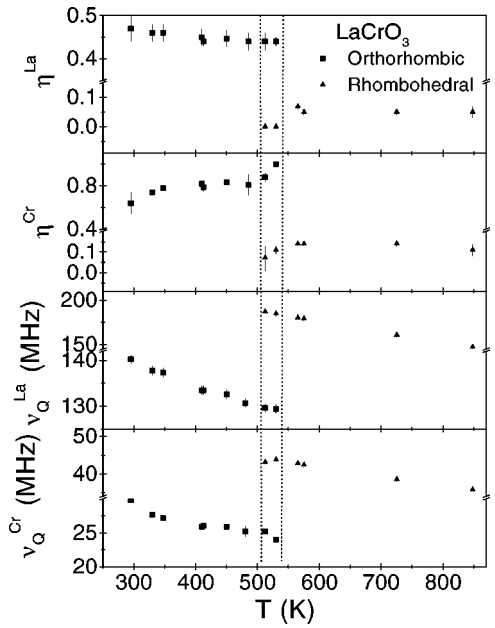

FIG. 6. The temperature dependence of fitted hyperfine parameters (η and ν_Q) of ^{111}Cd at La and Cr sites in $LaCrO_3$. The dotted lines show the region of the coexistence of both orthorhombic and rhombohedral phases.

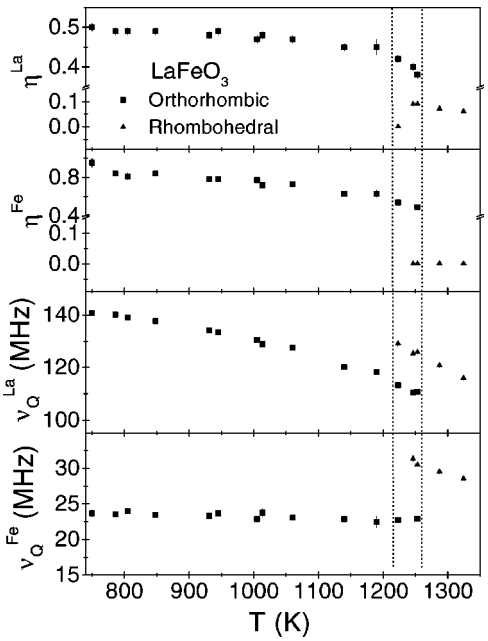

FIG. 7. The temperature dependence of fitted hyperfine parameters (η and ν_Q) of ^{111}Cd at La and Cr sites in $LaFeO_3$. The dotted lines show the region of the coexistence of both orthorhombic and rhombohedral phases.

$\sim$44% and to $\sim$70% for La and Cr sites. The Fourier spectra indicated coexistence of two phases in the temperature range 512–530 K, therefore the data were fitted with two different sets of quadrupole interaction parameters. The rhombohedral phase is stable above 530 K up to at least 848 K, the highest temperature at which the measurements were performed. A relatively narrow frequency distribution ($\delta \sim 4\%$) is observed for the probes at the Cr site over the measured temperature range except at 295 K where δ is $\sim$10%. As the Néel temperature of $LaCrO_3$ is close to room temperature, the influence of a small magnetic hyperfine field is most probably responsible for this increase in the frequency distribution. The frequency distribution at the La site is very small: $\delta < 2\%$. It is interesting to note that ν_Q decreases slowly but almost linearly in both phases with increasing temperature. This roughly corresponds to an earlier observation of the linear thermal expansion of the $LaCrO_3$ lattice[13] above and below the structural phase-transition temperature. It is further observed that the relative populations of the probe nuclei at La and Cr remain essentially constant over the entire temperature range 295–848 K.

The temperature dependence of the hyperfine parameters of $LaFeO_3$, shown in Fig. 7, has similar features as in the case of $LaCrO_3$. There are, however, a few notable differences. The onset of the orthorhombic-to-rhombohedral structural phase transition occurs around 1223 K and the two phases coexist in the temperature region of 1223–1253 K. While the asymmetry parameter for the La site remains nearly constant, $\eta \sim 0.5$, the value for the Fe site decreases gradually from $\sim$1.0 to $\sim$0.6 in the temperature range 750–1220 K. The decreasing of the η value for the Fe site indicates that the distortion of the FeO_6 octahedra in the orthorhombic phase is somewhat less (the FeO_6 octahedron is more relaxed) at higher temperatures. The asymmetry parameters for both sites drop almost to zero at about 1223 K and remain at this value in the rhombohedral phase up to the highest measured temperature of 1324 K. This is once again consistent with the threefold axial symmetry at La as well as at Fe sites in the rhombohedral phase of the $LaFeO_3$ perovskite. Although the interaction frequencies for both sites increase suddenly around the phase-transition temperature, the jump ($\sim$14% for the La site and $\sim$35% for the Fe site) in the values of ν_Q is not as dramatic as in the $LaCrO_3$ perovskite. For the La site, the frequency distribution parameter δ remains very small (1–2%) over the whole temperature range 750–1324 K and the site fraction is essentially constant except at higher temperature where it decreases. In the orthorhombic phase, the La site frequency reduces gradually from $\sim$140 MHz at 800 K to $\sim$110 MHz at 1253 K with increasing temperature, jumps to a higher value of $\sim$125 MHz at the phase-transition region of 1223–1253 K, and then continues to decrease almost linearly with temperature in the rhombohedral phase. In contrast, the quadrupole frequency for the Fe fraction changes very little in the orthorhombic phase but has much wider distribution $\delta \sim 5$–8%. In the rhombohedral phase, the quadrupole frequency is characterized by an almost axially symmetric electric-field gradient with very narrow distribution. The quadrupole frequency in this phase decreases linearly up to the highest measured temperature.

Figure 8 shows the PAC spectra of $LaCrO_3$ and $LaFeO_3$ samples below their respective magnetic transition temperatures. While the spectra of $LaFeO_3$ show well-defined combined electric-quadrupole and magnetic dipole interactions from which the magnetic hyperfine fields can be deduced (see inset of Fig. 8), the spectra of $LaCrO_3$ have a strong

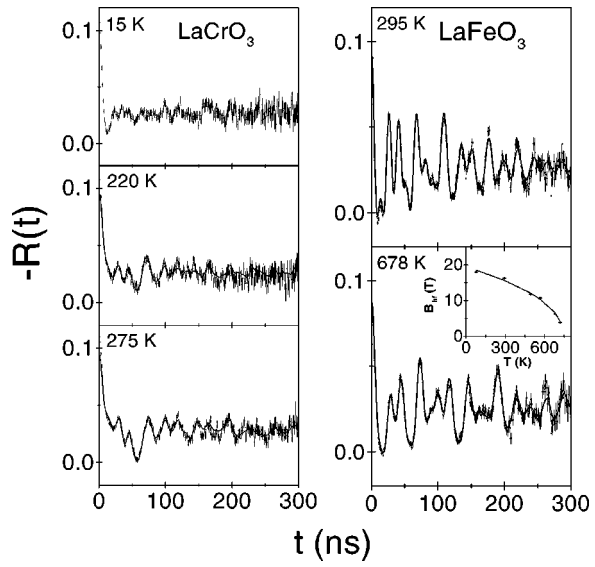

FIG. 8. Perturbation functions $R(t)$ of the ^{111}Cd probe in $LaCrO_3$ and $LaFeO_3$ below their respective Néel temperatures. All spectra were fitted with a two-site model of combined electric-quadrupole and magnetic dipole interactions. The inset shows the variation of the magnetic hyperfine field at the Fe site in $LaFeO_3$ as a function of temperature.

damping below 220 K that continues up to 15 K. The observed damping reflects a wide distribution in the observed hyperfine field and it was not possible to perform a precise analysis of the data to deduce unique hyperfine parameters below 220 K. Using fixed quadrupole frequencies ν_Q for the Cr site, extrapolated from the data given in Fig. 6, we analyzed the PAC spectra of $LaCrO_3$ at 275 and 220 K and obtained the Larmor frequencies ω_L as 10(1) and 17(4) Mrad/s, respectively, with a relatively wide distribution. The deduced hyperfine magnetic fields are 0.67(7) and 1.1(3) T at 275 and 220 K, respectively.

IV. DISCUSSION

A. Electric-field gradient

Since there is no formal charge difference between In^{3+} and La^{3+} and Cr^{3+} and Fe^{3+} we rule out the possibility that the EFG's at the La and Cr(Fe) sites in $LaCrO_3$($LaFeO_3$) perovskites are due to a trapping of defects. Furthermore, the observation of only a small frequency distribution in all cases indicates that the probe atoms occupy mostly substitutional positions and are relatively free from point defects. This enabled us to measure accurately the interaction frequencies and hence the EFG's.

The large EFG at the La site comes mainly from 12 surrounding O^{2-} ions forming a dodecahedra with four longer (La-O_1) and eight shorter (La-O_2) bonds. In contrast, the EFG's at Cr(Fe) sites are due only to six surrounding O^{2-} ions forming an octahedron and distributed in two planes with two Cr(Fe)-O_1 bonds in one plane and the remaining four Cr(Fe)-O_2 bonds in another plane (see Fig. 2), leading to a smaller contribution to the EFG. Since the La-O_1(La-O_2) bonds are coupled with Cr(Fe)-O_2[Cr(Fe)-O_1] bonds, any change in La-O bond length will affect the CrO_6(FeO_6) octahedron symmetry and vice-versa. It has been observed[14] that an increase in the temperature does not modify all bond lengths in dodecahedra and octahedra by the same amount: while some of the bonds increase with increasing temperature, others decrease. The EFG at the cation sites will, therefore, be determined by the contributions from all of these variations in bond lengths. It was pointed out that within errors, the quadrupole frequencies at La and Cr(Fe) sites decrease linearly in the rhombohedral phase over the measured temperature range, indicating that the La-O bond length and the corresponding tilting and twisting of CrO_6(FeO_6) octahedron smoothly change with temperature. On the other hand, in the orthorhombic phase, the decrease in the Cr site frequency with temperature is slower than at the La site and the Fe site frequency is almost temperature independent. It appears that, while the changes in the Fe-O bond lengths are not sufficient to produce the effective change in EFG with temperature, they are sufficient to produce the observed decrease in the asymmetry parameter. In the orthorhombic $LaFeO_3$ perovskite, we expect the observed decrease in the EFG at the La site with increasing temperature due to a decrease in the distortion of the LaO_{12} dodecahedra, and as a consequence a decrease in the distortion of FeO_6 octahedron. The observed decrease in the asymmetry parameter to nearly zero and an increase in the EFG values for the ^{111}Cd probe nuclei at La and Cr(Fe) sites near the structural phase-transition temperature provide microscopic evidence that the local point symmetry of the crystal has changed.

TABLE I. Experimental values of V_{zz} and η determined at room temperature for $LaCrO_3$ and $LaFeO_3$ perovskites compared to the values calculated by a point-charge model (PCM) for a distorted orthorhombic structure.

Compound	Site	$\lvert V_{zz}^{exp}\rvert$ (10^{21} V/m^2)	η^{exp}	V_{zz}^{PCM} (10^{21} V/m^2)	η^{PCM}
$LaCrO_3$	La	7.0(9)	0.47(3)	2.5	0.53
	Cr	1.5(2)	0.64(9)	23.5	0.92
$LaFeO_3$	La	7.3(9)	0.43(2)	4.2	0.45
	Fe	1.3(2)	0.95(5)	16	0.43

Point-charge model (PCM) calculations of V_{zz} and η were performed for both perovskites in the orthorhombic phase. Formal charges of $+3$ and -2 were assigned to La, Fe, Cr, and oxygen ions, respectively. The lattice sum was performed numerically to within a sphere of radius of 100 Å with a probe atom at the origin. The lattice parameters and the atomic positions were taken from the Rietveld analysis of the samples. The resulting value of V_{zz}^{lat} was then multiplied by $(1-\gamma_\infty)$ where $\gamma_\infty = 29.27$ is the known Sternheimer antishielding factor for Cd to obtain the EFG at the nuclear site $V_{zz}^{PCM} = (1-\gamma_\infty)V_{zz}^{lat}$. The results of the PCM calculation of V_{zz} and η are shown in Table I for La and Cr(Fe) sites in

both perovskites. The experimental results are included in this table for comparison. While the agreement between the experimental and calculated values of asymmetry parameters η is reasonable only for the La sites, the agreement for V_{zz} is quite poor. Whereas the V_{zz} values for La sites are found to be underestimated by a factor of about 2, the values for Cr and Fe sites are overestimated by a factor of more than 10. The disagreement between PCM calculations and experimentally observed EFG values indicates large contributions from covalent bonding. In a previous compilation[15] of EFG values on ^{111}Cd at cation sites for different types of oxides, a better agreement between the experimental V_{zz} and V_{zz}^{PCM} was obtained in cases where the cation-O^{2-} bond distance was greater than 2.1 Å . In the case of $LaCr(Fe)O_3$ perovskites, the La-O^{2-} and Cr(Fe)-O^{2-} bond distances range from 2.50 to 2.72 and 1.92 to 1.98 Å, respectively. Although the disagreement between experimental and calculated EFG values are larger in this work, we can conclude that basically a similar behavior is followed by $LaCr(Fe)O_3$ compounds. More elaborate electronic structure calculations may be required to correctly describe the effects of covalent bonding.

Recent PAC measurements have clearly shown that for perovskite compounds such as ABO_3 (A=Pb, Ba; B=Ti, Hf), the observed electric-quadrupole frequencies and asymmetry parameters change by a large amount from one phase to another.[16–18] We have observed similar trends near structural phase transitions in both compounds $LaCrO_3$ and $LaFeO_3$. Since the overall temperature dependence of ν_Q and η for both sites follows a steplike behavior, we characterize these phase transitions as step transitions. The observed structural phase transition in these compounds is not a first-order transition since two different sets of interaction frequencies at both sites appear to coexist near the transition temperature. This large temperature range of coexistence may be due to the fact that the polycrystalline sample consists of grains with varying sizes and the phase transformation involves volume change and, at a specific temperature near the transition, only a part of the grains may have completed the phase transformation, i.e., the local temperature at each grain with a different size is different. The fact that the probe nuclei at each atomic site are characterized by two sets of quadrupole frequencies near transition temperature clearly indicates that the probes reside in two types of grains differing in structure. Catchen, Hollinger and Rearick[18] have explained this type of coexistence by considering nucleation temperature within the powder specimen, where nucleation sites are related with point defects and their distribution is nonuniform.

B. Magnetic hyperfine interaction

The Cd^{2+} probe, formed in the decay of ^{111}In, substitutionally replaces the transition-metal ions Cr^{3+} or Fe^{3+} in $LaCrO_3$ and $LaFeO_3$, respectively, and is octahedrally surrounded by six oxygen anions and further by six transition-metal ions all belonging to the same sublattice. One should therefore expect a hyperfine magnetic field at the ^{111}Cd nucleus if spin density is transferred from the paramagnetic $Cr^{3+}(Fe^{3+})$ ions to the diamagnetic Cd^{2+} ion through

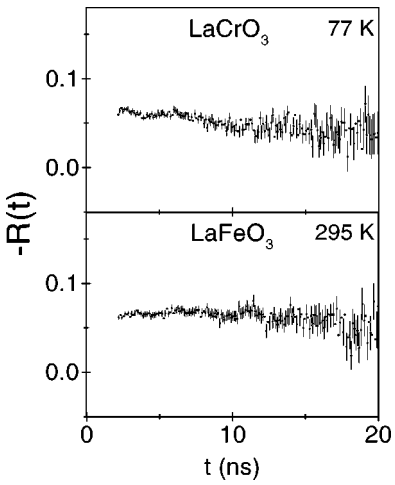

FIG. 9. Perturbation functions $R(t)$ of the ^{140}Ce probe in $LaCrO_3$ and $LaFeO_3$ below their respective Néel temperatures.

$Cr^{3+}(Fe^{3+})-O^{2-}-Cd^{2+}$ bonds. The transfer occurs through the spin polarization of the closed Cd^{2+} s shells by magnetic neighbors as well as through the overlap of the oxygen p orbital transferring unpaired spin density into the outermost Cd 5s orbital.[19] This interaction is analogous to the indirect Cr(Fe)-O-Cr(Fe) exchange interaction and the effective field is referred to as the supertransferred hyperfine magnetic field (SHMF).

Since orbitals with rotational symmetry around the bond axis transfer maximum spin density, these should be considered in the first place, e.g., e_g orbitals (d_{z^2} and $d_{x^2-y^2}$) in $Cr^{3+}(Fe^{3+})$, p orbitals in O^{2-}, and s orbitals in Cd^{2+}. In Cr^{3+} ($3d^3 \rightarrow t_{2g}^{3\uparrow} e_g^0$) the e_g orbitals are empty, therefore, the t_{2g} orbitals (d_{xy}, d_{yz}, d_{zx}), which have relatively small overlap with the orbitals of nearby oxygen or lanthanum ions, tend to form a localized t_{2g} ion core and transfer less spin density to Cd^{2+} orbitals via Cr^{3+}-O^{2-}-Cd^{2+} exchange bonds. As a consequence, the supertransferred magnetic hyperfine field at Cd^{2+} nuclei would be smaller in $LaCrO_3$ as compared to $LaFeO_3$ where maximum spin density is transferred to Cd^{2+} through the Fe^{3+}-O^{2-}-Cd^{2+} bond since e_g orbitals in Fe^{3+} ($3d^5 \rightarrow t_{2g}^{3\uparrow} e_g^{2\uparrow}$) have two spin ($\uparrow$) electrons. One does not expect any contribution from lanthanum ions towards the observed hyperfine field because these ions order magnetically below 10 K. The observed hyperfine magnetic field at the La site in both compounds is small ($\sim$0.3 T) as relatively small spin density is likely to be transferred to Cd^{2+} ions at La sites from the nearest $Cr^{3+}(Fe^{3+})$ ions. This is due to the fact that the $Cr^{3+}(Fe^{3+})-O^{2-}-La^{3+}$ exchange bond angle is approximately 90° and produces only a small overlap of oxygen p orbitals with s orbitals of Cd^{2+}.

The PAC spectra for $LaFeO_3$ and $LaCrO_3$ measured by using the $^{140}La \rightarrow {}^{140}Ce$ probe obtained below their respective Néel temperatures are shown in Fig. 9. Since the quadrupole moment of the 2083-keV 4^+ state of ^{140}Ce is known to be very small,[20] we expect to observe an almost pure magnetic dipole interaction at the La site. Unfortunately it was not possible to determine accurate values of the Larmor frequencies from these measurements as the observed modu-

lation period is very large compared to the time window for observation, the half-life (3.5 ns) of the intermediate state of the gamma cascade. We therefore estimated from computer simulation an upper limit of the Larmor frequency ω_L in both cases to be $\sim$20 Mrad/s and the corresponding hyperfine magnetic field to be of the order of 0.3–0.4 T. These results reconfirm our findings from the PAC measurements with $^{111}In \rightarrow {}^{111}Cd$ probes that the supertransferred hyperfine magnetic field at the La site in these perovskites is rather small. A visual inspection of the spectra in Fig. 9 shows that the slope for the $LaCrO_3$ curve is higher than that for the $LaFeO_3$. This is because of the fact that the 90° Cr^{3+}-O^{2-}-La^{3+} superexchange interactions are stronger than 90° Fe^{3+}-O^{2-}-La^{3+} superexchange interactions.[21]

As the orbital angular momentum is quenched due to the crystal-field potential of the oxygen octahedra,[22] the magnetic moments of Cr^{3+} and Fe^{3+} are due to spin only, with values of 3 and 5 μ_B, respectively. One should therefore expect that the resulting SMHF at ^{111}Cd probes on Cr^{3+} and Fe^{3+} sites are approximately in the same ratio, i.e., 3:5. The inset in Fig. 8 shows the temperature dependence of MHF at the Fe site in $LaFeO_3$, which follows the well-known power law $B_{hf}(T)=B_{hf}(0)(1-T/T_N)^{\beta}$ for magnetic materials yielding $B_{hf}^{Cd}(0)=19.4(4)$ T corresponding to a frequency $\omega_L(0)=285(5)$ Mrad/s and exponent $\beta=0.44(2)$. In order to compare the hyperfine field in both perovskites, we assumed that the temperature dependence of MHF at the Cr site in $LaCrO_3$ is approximately the same as for the Fe site in $LaFeO_3$ and follows the same power law. The deduced $B_{hf}^{Cd}(0)=2.4(3)$ T at the Cr site in $LaCrO_3$ is smaller by almost a factor of 8 than the corresponding value in $LaFeO_3$. It appears therefore that considerably less spin density is transferred to Cd^{2+} probes through the Cr^{3+}-O^{2-}-Cd^{2+} bond despite the fact that the exchange bond angles of 159° in $LaCrO_3$ and 164° in $LaFeO_3$ are nearly the same. These bond angles were calculated from the computer simulated structures using fitted parameters taken from the x-ray-diffraction measurements. One possible explanation could be that the *p* orbitals of oxygen are polarized as a result of charge transfer to unoccupied *d* orbitals of Cr^{3+} and the transfer of oxygen *p* electrons with spin ($\uparrow$) into the empty e_g orbital of Cr^{3+} predominates because of the strong intra-atomic interaction with the localized t_{2g} electrons ($\uparrow$), which leads to a negative spin density on the *p* orbital of oxygen.[23] The resulting spin density transferred to the diamagnetic Cd^{2+} ion will thus be much less compared to $LaFeO_3$ where the *d* orbitals of Fe^{+3} (t_{2g} and e_g) are half-filled.

V. CONCLUSION

The present PAC measurements in $LaCrO_3$ and $LaFeO_3$ perovskites have reconfirmed that in these compounds the $^{111}In \rightarrow {}^{111}Cd$ probe nuclei prefer to substitute both La and Cr(Fe) cation sites. The observation of only a narrow distribution of quadrupole frequencies is an indication that probe atoms occupy mostly substitutional positions in the lattice. The relative population of the probe atoms substituting La or Fe is found to be highly dependent on the sintering temperature of the sample. A higher sintering temperature leads to a larger La site occupation. Extensive PAC measurements, both above and below the Néel temperatures, have revealed important information on structural as well as magnetic properties of both perovskites. The temperature dependence of the electric-quadrupole interaction in the paramagnetic region shows the presence of a phase transition from an orthorhombic to rhombohedral structure. The structural phase transition shows a steplike behavior and is characterized by the coexistence of orthorhombic and rhombohedral phases between 512 and 530 K in $LaCrO_3$ and between 1223 and 1253 K in $LaFeO_3$. The PCM calculations of V_{zz} and the asymmetry parameter η for ^{111}Cd nuclei substituting La as well as Cr(Fe) sites were carried out for both compounds in the orthorhombic phase. The calculated values of V_{zz} are not in good agreement with the experimental results. The PAC measurements below the Néel temperature show the presence of magnetic ordering in both perovskites. The observed MHF at the ^{111}Cd probe substituting the Cr and Fe atom sites is believed to be due to the transfer of spin density from the paramagnetic ions Cr^{3+} and Fe^{3+} to the diamagnetic Cd^{2+} ion via the Cr(Fe)-O-Cd bond with the participation of an intermediate oxygen ion. The supertransferred magnetic hyperfine field at the Fe sites in $LaFeO_3$ was found to increase smoothly with decreasing temperature. Strong damping was observed in the perturbation functions for the $LaCrO_3$ sample below 220 K. The observed supertransferred MHF at the Cr site is much smaller than at the Fe site. PAC measurements with ^{140}Ce as well as ^{111}Cd probes also indicate only a small supertransferred MHF at the La site.

ACKNOWLEDGMENTS

Partial financial support for this research was provided by the Fundação de Amparo para Pesquisa do Estado de São Paulo (FAPESP). R.D. and A.C.J. thankfully acknowledge the financial support provided by FAPESP. We also wish to thank Dr. Jose A. H. Coaquira from IFUSP for his help in the magnetization measurements.

*On leave from SBS College of Engg. and Tech., Ferozepur-152001, India.

†Corresponding author. Email address: carbonar@curiango.ipen.br

[1] V. Goldschmidt, *Geochemistry* (Clarendon Press, Oxford, 1958).

[2] A. M. Glazer, Acta Crystallogr., Sect. B: Struct. Crystallogr. Cryst. Chem. **28**, 3384 (1972).

[3] S. Geller and P. M. Racah, Phys. Rev. B **2**, 1167 (1970), and references therein.

[4] T. Hashimoto, N. Matsushita, Y. Murakami, N. Kojima, K. Yoshida, H. Tagawa, M. Dokiya, and T. Kikegawa, Solid State Commun. **108**, 691 (1998), and references therein.

[5] T. Hashimoto, N. Tsuzuki, A. Kishi, K. Takagi, K. Tsuda, M. Tanaka, K. Oikawa, T. Kamiyama, K. Yoshida, H. Tagawa, and M. Dokiya, Solid State Ionics **132**, 181 (2000), and references therein.

[6] K. Tezuka, Y. Hinatsu, A. Nikamura, T. Inami, Y. Shimojo, and Y. Morii, J. Solid State Chem. **141**, 404 (1998), and references therein.

[7] T. M. Rearick, G. L. Catchen, and J. M. Adams, Phys. Rev. B **48**, 224 (1993).

[8] R. L. Rasera and G. L. Catchen, Phys. Rev. B **58**, 3218 (1998).
[9] J. Roth, M. Uhrmacher, P. de la Pressa, L. Ziegeler, and K. P. Lieb, Z. Naturforsch., A: Phys. Sci. **55**, 242 (2000), and references therein.
[10] G. L. Catchen, W. E. Evenson, and D. Allred, Phys. Rev. B **54**, R3679 (1996).
[11] S. E. Dann, D. B. Currie, M. T. Weller, M. F. Thomas, and A. D. Alrawas, J. Solid State Chem. **109**, 134 (1994).
[12] M. Eibschutz, S. Shtrikman, and D. Treves, Phys. Rev. **156**, 562 (1967).
[13] H. Hayashi, M. Watanabe, and H. Inaba, Thermochim. Acta **359**, 77 (2000).
[14] X. Liu and C. T. Prewitt, J. Phys. Chem. Solids **52**, 441 (1991).
[15] A. W. Carbonari, J. Mestnik-Filho, R. N. Attili, M. Moralles, and R. N. Saxena, Hyperfine Interact. **120/121**, 475 (1999).
[16] R. Alonso, A. Lopez, A. Ayala, and P. de la Pressa, J. Phys.: Condens. Matter **10**, 2139 (1998).
[17] M. Uhrmacher, V. V. Krishnamurthy, K. P. Lieb, A. Lopez-Garcia, and M. Neubauer, Z. Phys. Chem. (Munich) **206**, 249 (1998).
[18] G. L. Catchen, E. F. Hollinger, and T. M. Rearick, Z. Naturforsch., A: Phys. Sci. **51**, 411 (1996).
[19] H. H. Rinneberg and D. A. Shirley, Phys. Rev. Lett. **22**, 1147 (1973); Phys. Rev. B **13**, 2138 (1976).
[20] K. Królas and B. Wodniecka, H. Niewodniczandki Institute of Nuclear Physics, Kraków, Poland, Report No. 1644/OS-1993 (unpublished).
[21] J. B. Goodenough, *Magnetism and the Chemical Bond* (Wiley, New York, 1963), p. 157.
[22] Y. Tokura and N. Nagaosa, Science **288**, 462 (2000).
[23] I. S. Lyubutin, T. V. Dmitrieva, and A. S. Stepin, JETP **88**, 590 (1999).